EXPERIMENTAL INVESTIGATION OF AN IMPROVED EXHAUST RECOVERY SYSTEM FOR LIQUID PETROLEUM GAS FUELED SPARK IGNITION ENGINE

by

Habib GURBUZ* and Husameddin AKCAY

Department of Mechanical Engineering, Faculty of Engineering,
Suleyman Demirel University, Isparta, Turkey

Original scientific paper
DOI: 10.2298/TSCI150417181G

In this study, we have investigated the recovery of energy lost as waste heat from exhaust gas and engine coolant, using an improved thermoelectric generator in a liquid petroleum gas fueled spark ignition engine. For this purpose, we have designed and manufactured a 5-layer heat exchanger from aluminum sheet. Electrical energy generated by the thermoelectric generator was then used to produce hydrogen in a proton exchange membrane water electrolyzer. The experiment was conducted at a stoichiometric mixture ratio, 1/2 throttle position and six different engine speeds at 1800-4000 rpm. The results of this study show that the configuration of 5-layer counterflow produce a higher thermoelectric generator output power than 5-layer parallel flow and 3-layer counterflow. The thermoelectric generator produced a maximum power of 63.18 W when used in a 5-layer counter flow configuration. This resulted in an improved engine performance, reduced exhaust emission as well as an increased engine speed when liquid petroleum gas fueled spark ignition engine is enriched with hydrogen produced by the proton exchange membrane electrolyser supported by thermoelectric generator. Also, the need to use an extra evaporator for the liquid petroleum gas fueled spark ignition engine is eliminated as liquid petroleum gas heat exchangers are added to the fuel line. It can be concluded that an improved exhaust recovery system for automobiles can be developed by incorporating a proton exchange membrane electrolyser, however at the expense of increasing costs.

Key words: *liquid petroleum gas fueled spark ignition engine, waste heat recovery, thermoelectric generator, hydrogen production*

Introduction

In recent years, there has been increasing concern related with the emissions that cause global warming. Therefore, alternative technologies for generating electrical power and thermoelectric power emerge as promising green technologies [1]. Only 25% of the heat generated by fuel combustion is used to power vehicles with internal combustion engines, 40% of the energy is discarded to the atmosphere as exhaust gas while 30% of energy is transferred to engine coolant and 5% is consumed as a result of friction [2]. Heat energy lost through the exhaust system is

---

* Corresponding author; e-mail: habibgurbuz@sdu.edu.tr

higher than the heat energy lost through the engine cooling system or the lubricating oil. Using a thermoelectric generator (TEG), it is possible to produce electrical energy from waste heat energy discarded through the exhaust system. A TEG works as a heat engine, and produces electrical energy from heat energy, based on the principle of Seebeck effect [1]. The TEG have been used for power production in vehicles for several decades. They have the ability to recover waste heat directly and generate electricity without adding any load to the engine [3]. The efficiency of the consumed fuel in the internal combustion engine can be increased via a TEG. Also, TEG will help to increase fuel efficiency by reducing battery needs and increasing usable electrical energy for other electrical systems. The TEG can produce electricity in a short time by using the exhaust gas and engine coolant heat after an engine is started [4]. The key advantages of TEG for waste heat recovery are its simple structure, low maintenance requirements and safe use, since there is no rotating machinery in the system. There are disadvantages such as low conversion efficiency, high cost, and difficult system integration [5].

A TEG uses semiconductor materials (SEM), which are both of N-type and P-type connected in a series to boost the voltage [4]. The SEM offer an optimal combination of the seebeck coefficient, electrical resistivity, and thermal conductivity [6]. The TEG is made up of nonmoving parts made from SEM [7]. The figure of merit ZT describes material performance and it depends on the properties of thermoelectric materials (TEM). A thermoelement is made up of a pair of an N-type and P-type junctions and a module is made up of several thermoelement couples. The couples and their electrical interconnects are generally enclosed in an ceramic electrical insulator [4]. Bismuth telluride, lead telluride and silicon germanium are typically used in generator devices. The high cost of tellurium and germanium lead to the development of TEM [8]. The TEM formed from bismuth telluride are generally used for heating, cooling, and combined cooling [9]. Conversion efficiency of using a single module is relatively low. The use of thermoelectric generation, including several TEM, is an ideal application for conversion of waste heat energy to electrical energy [10]. The electrical needs of a typical automobile can be supplied by TEG, according to the result of a theoretical study [11]. The power generation efficiency of a TEG depends not only on the system design, but also on the TEM [12]. The optimum TEG electrical power output and conversion efficiency depends not only on TEM properties and dimensions but also on system-level electrical and thermal resistances [13]. Heat exchangers are required on both hot and cold sides for many applications of the TEG system. The heat transferred through the heat exchangers from the heat source along the TEM hot side is transferred to the cold side. Thus, the activity of the heat exchangers is affected directly by the temperature difference between the cold side and hot side [8]. The TEG performance is characterized by thermodynamic efficiency and the power density [14].

Conklin and Szybist [15] determined that only 10.4% of fuel energy is converted to useful work and also that the heat energy lost with exhaust gas is about 27.7%. Stobart and Weerasinghe [16] investigated the possibility of waste heat recovery in vehicles, and they found out that a 1.3 kW TEG output could potentially replace the alternator system of a small passenger vehicle. Stobart *et al*. [17] explored the potential of TEG in fuel saving for vehicles. They concluded that approximately 4.7% of fuel economy can be achieved. Birkholz *et al*. [18] produced a thermoelectric generator and were able to produce about 58 W direct current (DC) power in maximum conditions, using $FeSi_2$ elements. Ramade *et al*. [19] has achieved a system efficiency of 5.07% and TEG output power of 15.2 W at 3970 rpm engine speed using two layer heat exchanger in a 3-cylinder spark ignition (SI) engine with a 800 cm^3 cylinder volume. As a result of these studies, TEG technology emerged as a promising new technology in recovering waste heat from internal combustion engines.

In this experimental investigation the recovery of energy lost as waste heat through exhaust gases and engine coolant was investigated by using an improved TEG system in the liquid petroleum gas (LPG) fueled SI engine. A 5-layer heat exchanger with thermoelements (TE) was designed for waste heat recovery and manufactured from aluminum sheet material. The DC power produced by the TEG was used for production of hydrogen gas and engine charging. The hydrogen travels in a simple venturi along the intake manifold into the mixture of LPG-air as fuel enrichment.

Methodology (Experimental work)

Design of TEG

Chen *et al*. [20] notes that, the optimization of thermoelectric materials and systems for the design of a high-performance TEG had been the subject of much research. The TEG module consists of five rectangular heat exchangers, which are arranged in the form of a sandwich. The hot exhaust gas of the engine passes through the central heat exchanger before it is discharged into the atmosphere. The center exhaust heat exchanger, are designed according to the engine's maximum intake air flow, it has a inner volume of 1148 cm^3. This exchanger was manufactured from aluminum sheet material of 3 mm using aluminum welding. The inner volume of the center exhaust heat exchanger was separated into eight equal sections along the flow with a 2 mm aluminum sheet material for each TE line. The aluminum separator sheets caused a reduction of 78 cm^3 in the inner volume of the exhaust heat exchanger. The upper and lower engine coolant heat exchangers were positioned on the center exhaust gas heat exchanger. The engine coolant was circulated through the TEG by using nipple connectors and plastic hoses. The engine coolant heat exchangers which are designed according to the engine's maximum coolant flow, have inner volumes of 535 cm^3. The upper and lower LPG heat exchangers were positioned on the engine coolant heat exchangers. The LPG was circulated inside the TEG and then transferred to the intake manifold with nipple connectors and copper pipes. The LPG heat exchangers which are designed according to the engine's maximum LPG flow, have inner volumes of 334 cm^3. These heat exchangers were manufactured from 2 mm aluminum sheets using aluminum welding. Forty TEG1-1263-4.3 TE were positioned between the exhaust heat exchanger and the engine coolant heat exchangers. Twenty four TEC-12705 TE were positioned between the engine coolant heat exchangers and LPG heat exchangers. Thermal paste was used to minimize thermal contact resistance between the heat exchanger surface and TE modules. The side surfaces of the heat exchanger were covered with glass wool to minimize heat loss. The LPG and engine coolant was transferred to the heat exchanger from the distributors that was also used for thermocouple placement. The total weight of the manufactured TEG module is 13.656 kg. The pictures of the designed TEG are shown in fig. 1.

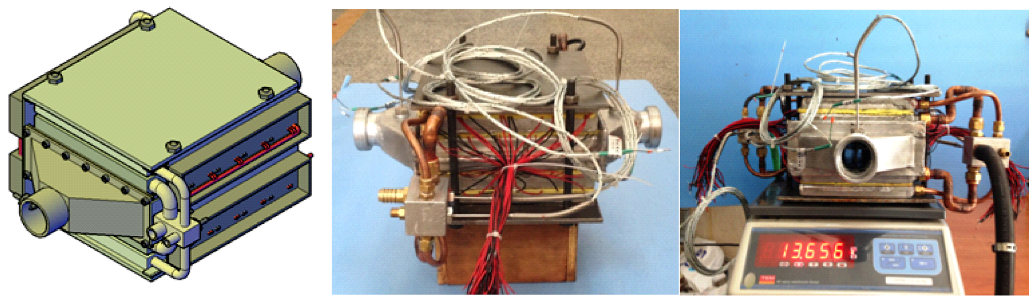

Figure 1. Pictures of designed TEG

Table 1. The technical specifications of the engine

Engine specifications	
Engine type	Lombardini LGW 523 MPI
Maximum rpm	6000 d/d
Maximum power	15 kW (5000 rpm)
Maximum torque	34 Nm (2150 rpm)
Bore stroke	72 mm 62 mm
Displacement volume	505 cm^3
Compression ratio	10.7:1
Operating temperature	78 °C-82 °C
Cooling circuit	30-80 l/h (1100-6000 rpm)
Volume of air flow	910 l/min (5000 rpm)

Experiment set-up

Experimental research was performed on the 2-cylinder SI engine. Table1 illustrates the technical specifications of the engine.

The LPG was injected into the engine at a pressure of about 1.5 bars by using the multi-point fuel injection technique. The e ngine was operated at the stoichiometric mixture ratio (ϕ = 1.0), 1/2 throttle position (TP) and six different engine speeds ranging between 1800-4000 rpm. The engine was coupled to a go-power-system D-100 water-brake dynamometer for loading. The engine speed was controlled by the change to load of water-brake dynamometer during the experiment. The spark timing and LPG injection time were controlled using a Motec-M4 engine control unit. The LPG and air flow rates were measured using New-Flow TSF03A10111 and TLF03A10111 types of thermal mass flow meters. The experimental set-up used in this work is shown in fig. 2.

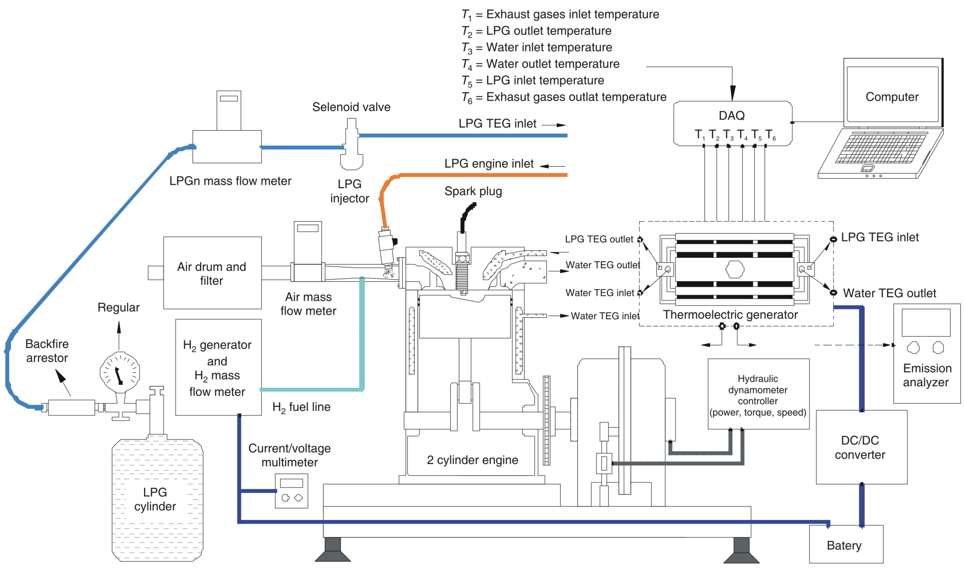

Figure 2. Schematic drawing of exoperimental set-up

The intake pressure was measured using a manifold-air-pressure (MAP) sensor. The temperature of engine coolant was measured at the engine block and it was recorded between 80-82 °C during the experiments. Intake air temperature and MAP was kept constant during experiments, respectively at 30 °C and 78 kPa. During the experiments, engine power, torque, and fuel consumption was recorded as the average of three consecutive measurements. A pressure regulator was used to maintain pressure of 1.5 bars for the LPG fuel line. For manifold injection of LPG, a LPG gas injector was used. A propane flashback arrester was added to stop flames from traveling up the fuel line. The LPG was supplied from the gas tank with about 6 bars of pressure. The exhaust gas, engine coolant and LPG inlet-outlet temperatures were measured using 6 K-type thermocouples. A data acquisition system (measurement computing USB-1616HS-4) was used to acquire inlet-outlet temperatures. Exhaust gases were measured using an IMR-FGA4000XDS-type emission analyzer. The maximum flow capacity of hydrogen generator is about 510 pure (99.999%) hydrogen at 4 bar operating on 260 W DC power. A proton exchange membrane (PEM) unit of electrolytic hydrogen generator operates with a maximum voltage of 3.5 V DC. The volume of hydrogen produced by the generator increases in correlation with the power supplied from the DC electric source. Hydrogen pressure and flow rate are adjustable with keys on the hydrogen generator.

The acquired data were used to calculate conversion efficiency of TEG as well as overall system efficiency. When temperature loss in the heat exchangers are ignored, the thermal power transferred to the TEG from the exhaust gas equals to:

$$Q_{\mathrm{ex}} = \dot{m}_{\mathrm{ex}} c_{\mathrm{p-ex}} (T_{\mathrm{ex-in}} - T_{\mathrm{ex-out}}) \tag{1}$$

$$\dot{m}_{\mathrm{ex}} = \dot{m}_{\mathrm{air}} + \dot{m}_{\mathrm{fuel}} \tag{2}$$

where Q_{ex} is the lost heat energy via exhaust gas, m_{ex} – the mass of exhaust gas, $c_{\mathrm{p-ex}}$ – the specific heat of the exhaust gas, $T_{\mathrm{ex-in}}$ – the exhaust gas inlet temperature, $T_{\mathrm{ex-out}}$ – the exhaust gas outlet temperature, m_{air} – the mass flow rate of air, and m_{fuel} – the mass flow rate of LPG. Specific heat ratio was taken into account according to the change in exhaust gas temperature at different engine operation modes. The instantaneous temperature values were used in calculations. The heat energy transferred from the exhaust gas to the engine coolant equals to:

$$Q_{\mathrm{h}} = \dot{m}_{\mathrm{h}} c_{\mathrm{p-h}} (T_{\mathrm{out}} - T_{\mathrm{in}}) \tag{3}$$

where Q_{h} is the heat energy of engine coolant in TEG, m_{h} – the mass flow rate of engine coolant, $c_{\mathrm{p-h}}$ – the specific heat of engine coolant, T_{in} – the engine coolant inlet temperature, T_{out} – the engine coolant outlet temperature. The conversion efficiency of TEG is defined in the eq (1):

$$\eta_{\mathrm{TEG}} = \frac{W_{\mathrm{TEG}}}{Q_{\mathrm{ex}}} \cdot 100 \tag{4}$$

where η_{TEG} is the recovery ratio of the electric power output (W_{TEG}) to the heat energy of the TEG (Q_{ex}). The overall system efficiency is defined in eq (5):

$$\eta_{\mathrm{SYSTEM}} = \frac{\Delta W_{\mathrm{Engin}}}{Q_{\mathrm{ex}}} \cdot 100 \tag{5}$$

where η_{SYSTEM} is the ratio of the increased engine power with the addition of hydrogen ($\Delta W_{\mathrm{Engine}}$) to the heat energy of the TEG (Q_{ex}). Lower heat value of the mixture (LHV_{mix}) taken into the engine was calculated for mixture of LPG + air and mixture of LPG + air + H_2 by using eq. (6):

$$LHV_{\text{mix}} \quad \frac{LHV_{\text{fuel}}\,\rho_{\text{air}}}{AFR} \tag{6}$$

where LHV_{fuel} is the lower heat value of fuel, ρ_{air} – the air density, and AFR – the air-fuel ratio.

Error analysis

Using eq. (7) the uncertainty in the computed values for engine performance and TEG parameters were also estimated from their respective uncertainties based on the Gaussian distribution:

$$\Delta R \quad \sqrt{\quad \frac{\partial R}{\partial x_1}\Delta x_1 \quad^2 \quad \frac{\partial R}{\partial x_2}\Delta x_2 \quad^2 \quad \ldots \quad \frac{\partial R}{\partial x_n}\Delta x_n \quad^2} \tag{7}$$

The error analysis is based on the accuracy of the measurement equipment which is given in tab. 2. The error rates in the measurement range of devices used in the experimental studies were taken into consideration in the error analysis.

Table 2. The error analysis based on the accuracy of the measurement equipment

Variable	Device	Accuracy	Parameters	2800 rpm	Error	[%]
BEP and BET	Go power syst. D-100	1.5 %	BEP	4.32 kW	0.0522 kW	1.21%
Engine speed	MotecM4 and Pick-up	6 rpm AR*	BTE	23.34%	0.168%	0.72%
Emission rate	IMR-FGA4000XDS	1 FS*	HC	237.8 ppm	2.05 ppm	0.86 %
Air flow rate	New-flow TSF03A10111	1.5% F 0.52**	BSFC	335.02 g/kWh	2.25 g/kWh	0.67%
LPG flow rate	New-flow TLF03A10111	1.5% F 0.33**	ϕ	1.0	0.0042	0.42%
Temperature	K type thermocouple	±1 °C	T_{ex}	240	1.87 °C	1.28%
Volt, ampere	Multimeter	0.5 V, A	DC power	18.25 W	0.137 W	0.75%

[*] AR: All range, FS: Full scale, [**]Accuracy of device in measurement range

Description of DC electrical power system

The inlet temperature of TEG was decreased 10 °C in the experimental studies with a simple heat exchanger which is positioned between the coolant inlet of the TEG and the coolant outlet of the SI engine. This means that the TEG coolant water tank would be placed behind vehicle's front grille which is cooled by the headwind. The experiment was divided into three sections according to the configuration of the heat exchanger and use of the TEG output power. In the first section, the effect of flow direction on the output power and conversion efficiency of TEG was investigated at six different engine speeds between 1800-4000 rpm. In the second section the effect of LPG heat exchangers on the output power and conversion efficiency of TEG was investigated at six different engine speeds between 1800-4000 rpm. The LPG was heated with an original LPG evaporator when LPG heat exchangers were not used. In the last section, the change in engine performance and emissions after hydrogen is added into mixture of LPG and air, was investigated. Also, the change in alternator activity was calculated when the output power of TEG is connected to the engine charging system in parallel. Forty TE were connected in series to the first heat transfer layer. Twentyfour TE were divided into six groups which are connected with each other in par-

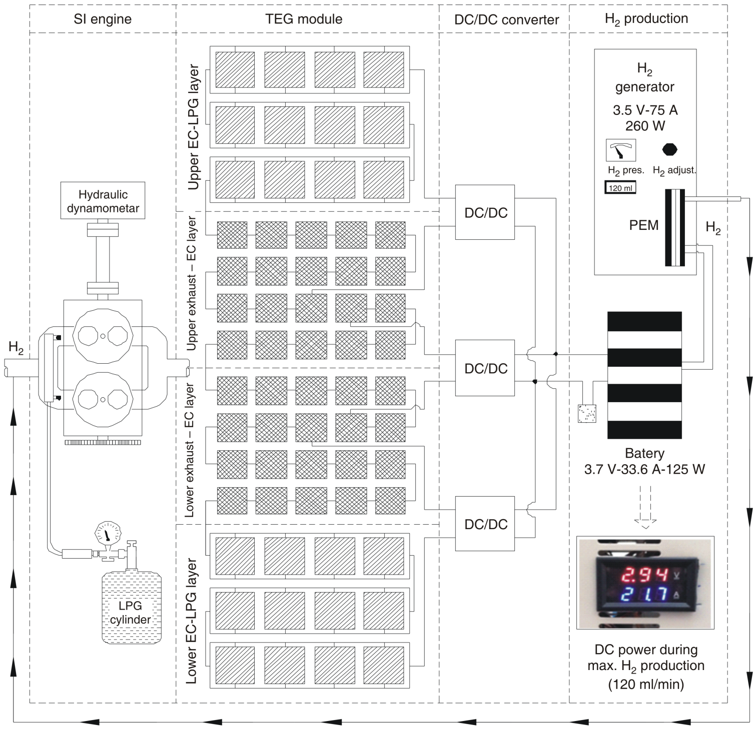

Figure 3. Block diagram of the TEG DC power generation system

allel to the second heat transfer layer. The six parallel groups were connected serially with the first layer. Thus, forty six TE modules were connected serially in order to increase the output voltage of TEG. Then, these forty six TE modules were divided into three groups as shown in fig. 3.

The DC electric energy produced by TEG was converted to 3.3 V with a three piece DC/DC converter which was connected to each other in parallel. During the experiment, DC/DC converters was used to charge the battery which has a 3.7 V and 33.6 A output capacity when fully charged. In the course of the experiment, only the PEM unit of the hydrogen generator was powered with a battery. The portion of battery capacity consumed here by the PEM was recharged using the output power of TEG. The output power of TEG was adjusted according to the engine running at 2000-4000 rpm. The amount of hydrogen that could be produced with the output power of TEG was calculated and was used in the engine experiments. The current and voltage produced by TEG was measured using a digital multimeter placed at the input of DC/DC converter. During the experiments, a fully charged battery was used to compensate for the efficiency loss in the DC/DC converter. A flow control valve was used to adjust the amount of hydrogen according to the determined output power of TEG at the engine operating speed. The flow and pressure rates of hydrogen were adjusted for engine speeds between 1800-3800 rpm, respectively, in the ranges of 54-118 ml per min and 1.1-1.3 bar. The hydrogen travels in a simple venturi through the intake manifold into the LPG-air mixture as fuel enrichment. Thus, hydrogen leakage in the intake line is minimised.

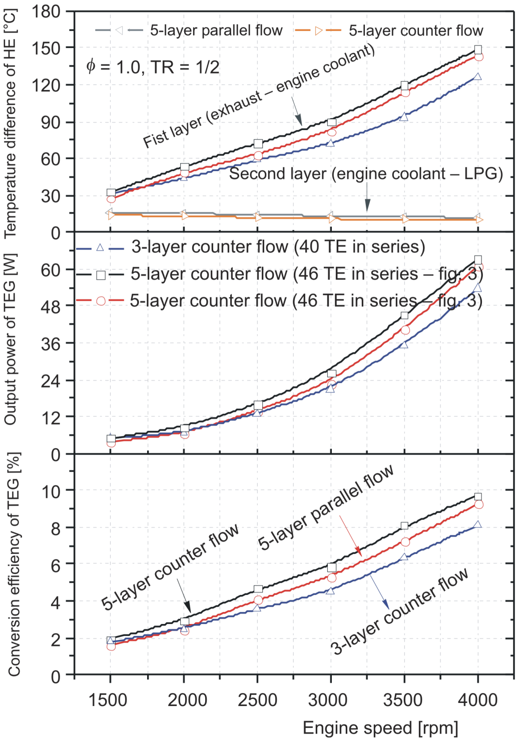

Figure 4. The effect of the TEG configuration on the TEG characteristics *vs.* the engine speed

Results and discussion

Optimal TEG configuration

Hendricks [21], indicated that the optimum ratio between the hot and cold sides of a system-level thermal resistance must be larger than 10-30 in order to achieve a maximum output power from TEG. Figure 4 shows the effect of the heat exchanger configuration on the TEG output characteristics *vs*. the engine speed.

The 5-layer counterflow configuration has produced a higher power output than the 5-layer parallel flow and 3-layer counterflow. The output power of the TEG was higher (7.2% at 2500 rpm – 13.2% at 4000 rpm) in the 5-layer parallel flow configuration as compared to the 3-layer counterflow, meanwhile also conversion efficiency of the TEG was as much as 1.1 unit higher at 2000-4000 rpm. The output power of TEG was approximately 13% higher at medium speeds (at 2500-3500 rpm) in the 5-layer counterflow configuration compared to the 5-layer parallel flow, meanwhile conversion efficiency of TEG was also 0.85 unit higher at 1500-4000 rpm. In this last configuration, as the engine speed increased, the output power of TEG has showed an increase in the range of 4.1-17.9% in the 5-layer counter flow configuration compared to the 3-layer counterflow configuration. The temperature difference (ΔT) between the heat exchanger surfaces in the first heat transfer layer increased due to the heat transferred to LPG, and as a result output parameters of TEG was improved. At higher speeds, the increased ΔT between heat exchanger surfaces resulted in an improvement in the output power of the TEG ranging between 0.2-9.6 watts in the 5-layer counterflow configuration compared to the 3-layer counterflow. Thus, conversion efficiency has increased 0.14-1.6 unit as the engine speed increased in the 5-layer counterflow configuration compared to the 3-layer counterflow. This is because, the configuration of counterflow has increased the rate of heat transfer and provided a uniform temperature difference between the hot surfaces and the cold surfaces along the heat exchangers. These results show that the configuration of heat exchanger and the specifications of exhaust gas have a significant effect on the output power of TEG. The configuration of high efficiency heat exchanger plays a key role in recovering higher heat energy from the exhaust gas.

Figure 5 shows temperature variations (*i. e*., inlet, outlet, and surface) in the heat exchangers (*i. e*., exhaust, engine coolant, and LPG) at 1500-4000 rpm. The temperature decrease throughout the exhaust line in TEG is mainly due to convective heat transfer from exhaust gas to the walls, as shown in fig. 5(a). The level of temperature decrease changed between 50 to 61 °C depending on engine speed. The surface temperature of heat exchangers has been lower than the temperature of the inlet-outlet of exhaust gas depending on the heat transfer coefficient of wall material and the flow speed of exhaust gas. The temperature of the engine coolant

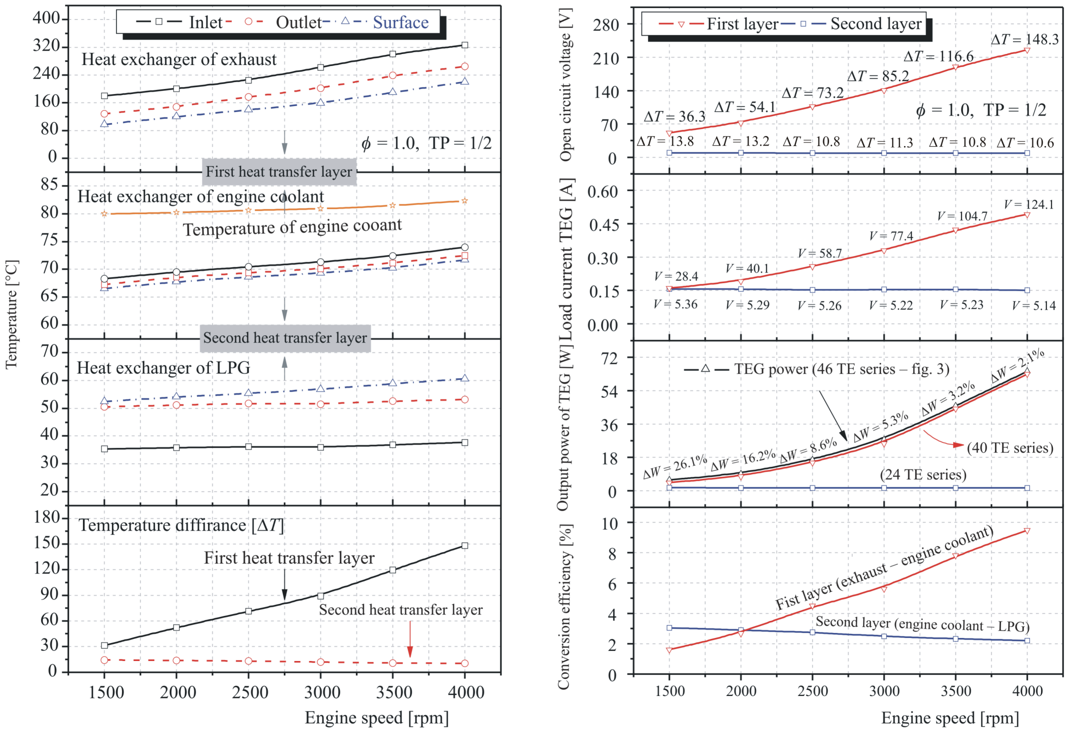

Figure 5. The variartion of temperatures in the heat exchangers *vs.* engine speed (a), and the variation of the output parameters of TEG *vs.* the engine speed for 5-layer counterflow (b)

decreased throughout the heat exchanger in TEG. This result can be explained with the heat transfer from the hot engine coolant to the cold LPG. Kumar *et al.* [22], showed that the temperature difference between the hot plate and the cold plate plays a major role in the functioning of the TEM. The LPG heat exchangers contributed to increase of TEG output power by maintaining the temperature difference between exhaust and engine coolant, as shown in fig.4. In addition, the heat transfer from the TEG to the LPG, has resulted in an increase in the output parameters of the engine by providing better combustion conditions. A TEG power increases with the square of the Δt applied across it [23]. Figure 5(b) illustrates the variation of output parameters of TEG *vs*. engine speed. The output power and conversion efficiency of TEG has increased as the surface temperature difference (ΔT) increased due to the rise in exhaust gas temperature in correlation with the rise in engine speed. TEG has yielded a maximum output power of 63.18 W at a ΔT of 148.3 °C at 4000 rpm. The LPG heat exchangers improved the maximum power generated in the TEG by 17.9%. The Δt between hot and cold surfaces of the TEG has increased as the engine speed increased. The conversion efficiency of TEG increased from 1.6% at 1500 rpm, to 9.4% at 4000 rpm in the first heat transfer layer, while decreasing from 3.1% at 1500 rpm to 2.2% at 4000 rpm in the second heat transfer layer. The results of this show that the power generated by the TEG is a function of the mass flow rate of hot and cold fluids governed by the resistance of thermoelectric modules and engine characteristics (speed and load).

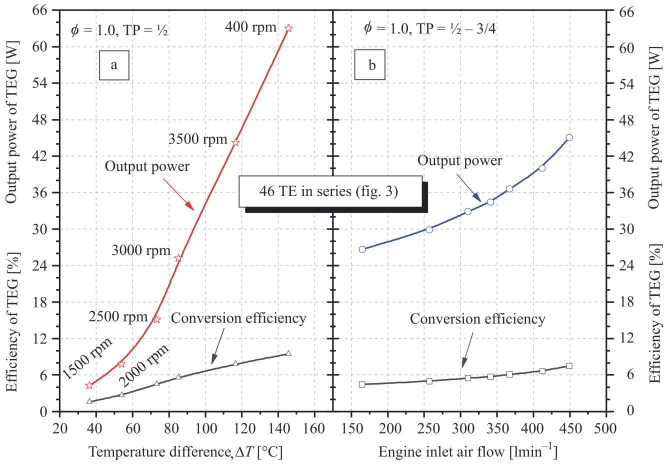

Figure 6. The effect of temperature difference (Δ*T*) and inlet air flow on the output power and conversion efficiency of TEG

The effect of ΔT on the output power and conversion efficiency of TEG is shown in fig. 6(a). These tests were performed by varying the engine speed and applying different dynamometer loads for TP of 1/2.

The output power and conversion efficiency of TEG has increased linearly as the ΔT between the heat exchanger surfaces increased. The output power of TEG increased 59 W as the temperature difference (ΔT) between the heat exchanger surfaces rose from 36 °C to 146 °C, meanwhile, conversion efficiency has increased 5.9% depending on the output power of TEG. The output power and conversion efficiency of TEG has increased along with engine inlet air flow. Results of tests performed by varying the engine speed for TP range of 1/2 -3/4 under constant dynamometer load is given in fig. 6(b). The output power of TEG has increased approximately 69%, while the conversion efficiency of TEG has increased 3.1%, when the intake air flow increased by 37%. The output power of TEG has increased depending on the heat energy passed per unit time on the TE modules, as the volume of exhaust gas involved in the heat transfer increased in parallel to air intake. These results suggest that the output power of TEG is a function of mass flow and ΔT in the TEG.

Optimal use of the TEG output power

Hydrogen possesses properties that positively affect the flame speed, flammability limits, and engine performance, making hydrogen a uniquely suitable fuel additive [24]. The increased flame speed with added hydrogen allows for combustion to occur more quickly at a given equivalence ratio [25]. The faster reaction rates of the H_2-O_2 mechanism also allows for reactions to occur in a shorter amount of time, decreasing the burn duration [26]. When hydrogen is added to a hydrocarbon fuel, both theoretical and experimental studies reveal that the hydrogen leads to an increase of H, O, and OH radical mole fractions, a faster chain branching and decreased burn duration [27, 28]. The characteristics of LPG and hydrogen are listed in tab. 3.

As shown in tab. 3, hydrogen has favorable combustion characteristics which can enhance flame stability when mixed with LPG fuels. An analysis of the properties of hydrogen and LPG shows that it is possible to obtain performance increase, fuel economy and emission reductions with the addition of hydrogen to the LPG fueled engine. In general, there is an increase in engine performance with the use of hydrogen in the dual-fuel mode, and a significant reduction in polluting emissions [29]. Kumar [30], showed results for a hydrogen-enriched engine that uses LPG as fuel which provided an increase in the engine performance and reduction of emissions. In this paper, the tests were conducted by varying the engine speed along with different dynamometers load for throttle opening of 1/2. At first, test results for engine operating on only LPG fuel was obtained at determined engine speeds, and then experiments were performed by making new measurements with the opening of the hydrogen fuel line. Fuel consumption of the

Table 3. Characteristics of LPG and hydrogen [29]

	C_4H_{10}	H_2
Theoretical AFR	15.5	34.3
Lower heat value [MJkg^{-1}]	45.84	120
Flammability limits	0.4-1.7	0.12-10.12
Density [kgm^{-3}]	2.64	0.0899
Adiabatic flame temperature [°C]	1990	2384
Turbulent burning velocity [ms^{-1}]	0.4	1.7
Autoignition temperature [°C]	585	450
Quenching distance [mm]	1.8	0.6
Minimum ignition energy [mJ]	0.36	0.02

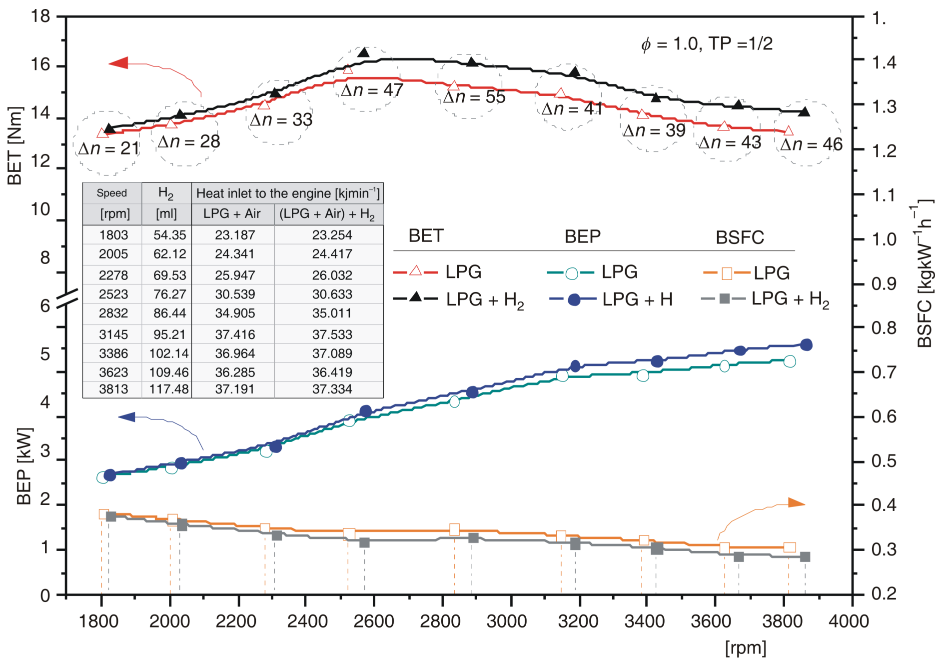

Figure 7. The variation of BEP, BET, and BSFC *vs.* engine speed

engine was determined by the increase in engine power due to added hydrogen to the constant fuel amount and this was represented as specific fuel consumption. The variation of brake engine power (BEP), brake engine torque (BET), and brake specific fuel consumption (BSFC) with engine speed is shown in fig. 7.

The BEP, BET, and BSFC improved at a rate of 1.5-6.6% as the engine speed increased with the addition of hydrogen, while the engine speed increased 21-55 rpm with the addition of hydrogen. While the maximum BEP value obtained on LPG has been 5.25 kW at 3813 rpm, BEP reached 5.62 kW, and the engine speed increased 46 rpm when hydrogen is added. There are two reasons for this increase, faster flame speed and higher specific energy of hydrogen led to shorter burn duration and better work transfer to the piston. These results could be explained by the improvement in the combustion process due to the closer extinction of the flame to combustion chamber walls by low quenching distance of hydrogen. Lower heat value of mixture (LHV_{mix}) has relatively increased to the range of 67-143 j per min when hydrogen was added gradually as the engine speed increased. The heating value and combustion speed of the mixture, partially enriched with hydrogen supplement, has improved and therefore engine performance parameters increased. Especially high combustion speed (hydrogen has four times higher burning velocity) and quenching distance of hydrogen has contributed to the creation of ideal combustion conditions while reducing the cycle losses. Choi *et al*. [31], described that BEP and thermal efficiency decrease with the increase of hydrogen supplement rate. Furthermore, the oxygen amount decreases around the rich and stoichiometric conditions with the increase of hydrogen supplement rate, and thus increasing CO. In this study, engine performance was increased thanks to the relative improvement in combustion conditions with low hydrogen supplement. Thus, the negative engine operating conditions, which occur due to insufficient oxygen amount in mixtures with high hydrogen supplement, has been avoided.

The LPG fueled SI engine enriched with hydrogen can be essentially characterised with low emissions and reduction of backfire for hydrogen engine [20]. The direct effects of the hydrogen addition on the turbulent flame speed, quenching distance, chemical kinetics and flammability limits of a fuel-oxidant mixture, can be evaluated together in terms of engine output parameter and exhaust emission.

The variation of exhaust emissions *vs*. engine speed can be observed in fig.8. Figure 8 shows a decrease in CO and HC emissions, as the hydrogen supplement has improved charge-mixture oxidation, and contributed to the conversion of the perfect combustion gas CO_2 of the carbon content in the fuel. Combustion temperature increased when hydrogen was added, due to hydrogen's higher specific energy density, resulting in increased NO_x emissions. The hydrogen addition led to a reduction in un-burnt HC and CO emissions, respectively of 8% and 4% on average at 1800-3900 rpm. Nevertheless CO_2 and NO_x emissions have increased with the added hydrogen, respectively 1% and 4%. The reduction of emissions (*i. e.*, HC and CO) can be explained with the improvement in the engine's thermal efficiency as a result of improved combustion in the cylinder. When hydrogen was added into the mixture of LPG and air, the combustion temperature increased due to hydrogen's higher specific energy density, resulting in increased NO_x emissions. The maximum value of NO_x rose from 1137 ppm at 3386 rpm to 1183 ppm at 3423 rpm when the hydrogen is added.

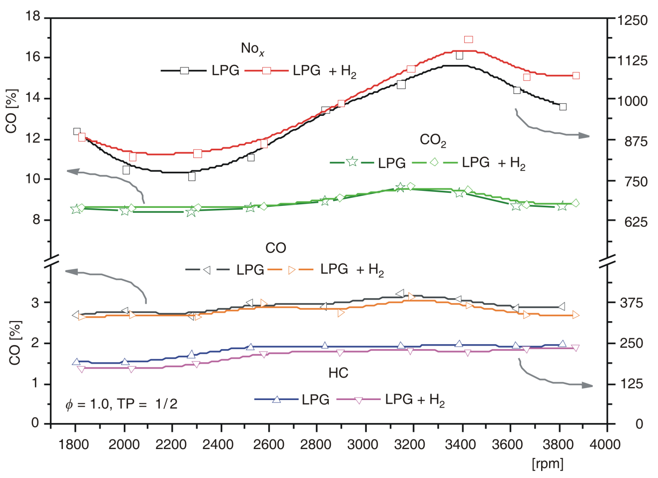

Figure 8. The variation of exhaust emissions vs. engine speed
(for color image see journal web site)

Figure 9 illustrates the variation of the overall system efficiency and conversion efficiency *vs.* engine speed. Overall system efficiency increases rapidly up to 2500 rpm, then slowly reaches 4000 rpm. The variation of the curve can be characterised with the effect of the change in the hydrogen production amount on the engine performance according to the output power of TEG . This positive result was obtained thanks to the increase in brake engine power as a result of the improvement of the brake thermal efficiency with the addition of hydrogen. The maximum overall system efficiency has been increased up to 56.5% with the conversion efficiency of 9.7% at an engine speed of 4000 rpm.

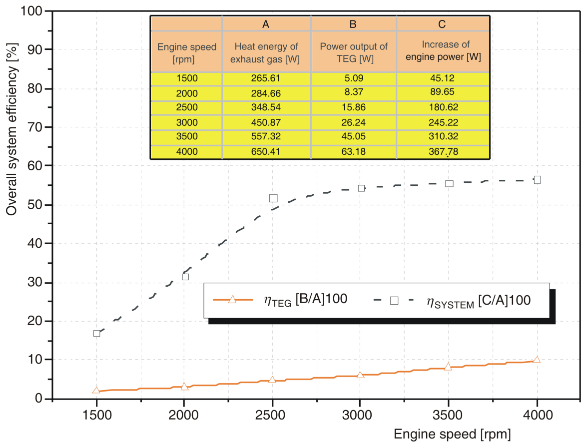

Figure 9. The variation of the conversion efficiency and overall system efficiency *vs.* engine speed

Bigger alternators are required to meet the high electricity demand of modern automobile systems. The electric power of engine charging system was measured during tests. Figure10 shows the possible reduction in the alternator activity if the output power of TEG was fed in to the charging system. When the electrical power produced by TEG is used in the charging system, the activity of the alternator can be decreased at a rate of 2.4-13.2% as the engine speed increases. It is possible to say that an improved exhaust recovery system for automobiles can be developed by producing hydrogen with that high energy, meanwhile set-up costs will be higher.

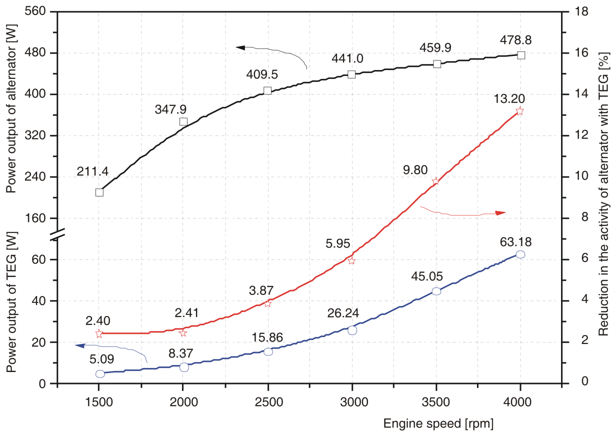

Figure 10. The state of engine charging system with electrical energy produced by TEG

Conclusions

This paper investigated the recovery of lost heat from the exhaust and engine coolant by using TEG in a LPG SI engine. The experiment results are summarised as follows.

The 5-layer counterflow configuration produced a higher TEG output power than the 5-layer parallel flow and 3-layer counterflow. As the engine speed increased, the increase in ΔT resulted in a 0.2-9.6 W improvement in the output power of TEG in the 5-layer counterflow configuration compared to the 3-layer counterflow. Thus, the value of conversion efficiency increased 0.14-1.6 unit as the engine speed increased in the 5-layer counterflow configuration compared to the 3-layer counterflow. The maximum output power of TEG increased by 17.9%

thanks to the use of the LPG heat exchanger. Results indicate that the 5-layer counterflow TEG design is capable of producing an 63.18 W output power at an ΔT of 148.3 °C and an engine speed of 4000 rpm.

With the addition of hydrogen produced by PEM electrolysis powered by TEG to the engine, a 1.5-6.6% increase in the BEP, BET, and BSFC and a 21-55 rpm increase in the engine speed was observed at 1500-4000 rpm. While the maximum BEP value recorded on LPG was 5.25 kW at 3813 rpm, when hydrogen is added, BEP reached a value of 5.62 kW and the engine speed increased 46 rpm. Furthermore, hydrogen supplement led to a reduction of un-burnt HC and CO emissions, respectively, 8% and 4%, while CO_2 and NO_x emissions has increased, respectively, 1% and 4%.

The overall system efficiency of TEG increased as high as 56.5% with a conversion efficiency of 9.7% at an engine speed of 4000 rpm when it is used with 5-layer heat exchanger and PEM electrolysis unit at the LPG-fueled SI engine.

This study reveals that an improved exhaust recovery system for automobiles can be developed by producing hydrogen with the energy generated, but at the expense of higher set-up costs. Also this eliminates the necessity to use an evaporator for a LPG-fueled SI engine when LPG heat exchangers are added to the fuel line. Furthermore, electricity production can be further increased with the use of thermoelectric modules and the exhaust energy recovery can be improved with design of better heat exchangers.

Acknowledgment

The authors acknowledge the financial support provided for this work by TUBITAK under contract number 113M578.

Nomenclature

$c_{p\text{-}h}$ – specific heat of engine coolant, [kjkg^{-1}K^{-1}]
$c_{p\text{-}ex}$ – specific heat of exhaust gas, [kjkg^{-1}K^{-1}]
HC – hydrocarbon
ICE – internal combustion engine
LHV_{mix} – lower heat value of mixture, [kjkg^{-1}]
LHV_{fuel} – lower heat value of fuel, [kjkg^{-1}]
$\dot{m}_{air}$ – mass flow rate of air, [kgs^{-1}]
$\dot{m}_{fuel}$ – mass flow rate of LPG, [kgs^{-1}]
$\dot{m}_{h}$ – mass flow rate of engine coolant, [kgs^{-1}]
$\dot{m}_{ex}$ – mass of exhaust gas, [kgs^{-1}]
NOx – nitrous oxide
Δn – engine speed increase, [dd^{-1}]
T_{in} – engine coolant inlet temperature, [K]
$T_{ex\text{-}in}$ – exhaust gas inlet temperature, [K]
$T_{ex\text{-}out}$ – exhaust gas outlet temperature, [K]
T_{out} – engine coolant outlet temperature, [K]
ΔT – temperature difference, [K]
Q_{ex} – heat lost energy by exhaust gas, [W]
Q_{h} – heat energy of engine coolant in TEG, [W]
Q_{LPG} – transferred heat energy to LPG, [W]
W_{TEG} – electric power output, [%]
ΔW – TEG ouput power increase, [W]
ΔW_{Engine} – variation of engine power, [W]

Greek symbols

η_{SYSTEM} – overall efficiency, [%]
η_{TEG} – conversion efficiency, [%]
ρ_{air} – density of air, [kgm^{-3}]
ϕ – equivalence ratio

Acronyms

AFR – air-fuel ratio
BEP – brake engine power
BET – brake engine torque
BSFC – brake specific fuel consumption
DC – direct current
EC – engine coolant
HE – heat exchanger
LPG – liquid petroleum gas
MAP – manifold air pressure
SEM – semiconductor materials
SI – spark ignition
TE – thermoelement
TEG – thermoelectric generator
TEM – thermoelectric materials
TP – throttle position

References

[1] Rowe, D. M., Thermoelectric Waste as a Renewable Energy Source, *International Journal of Innovations in Energy Systems and Power, 1* (2006), 1, pp. 13-23
[2] Yu, C., Chan, K. T., Thermoelectric Automotive Waste Heat Energy Recovery Using Maximum Power Point Tracking, *Energy Conversion and Management, 50* (2009), 6, pp. 1506-1612
[3] Rowe, D. M, *Thermoelectrics Handbook Macro to Nano*, CRC Press, Taylor & Francis Group, New York, USA, 2006
[4] LeBlanc, S., Thermoelectric Generators: Linking Material Properties and Systems Engineering for Waste Heat Recovery Applications, *Sustainable Materials and Technologies, 1* (2014), 2, pp. 26-35
[5] Yang, J., Potential Applications of Thermoelectric Waste Heat Recovery in the Automotive Industry, *Proceedings*, 24th International Conference on Thermoelectrics Clemson, S. C. USA, 2005
[6] Alexander, B., *et al*., Alphabet Energy: Thermoelectrics and Market Entry, California Management Review, 55 (2012), 1, pp. 149-160
[7] Shawwaf, A., Optimization of the Electrical Properties of Thermoelectric Generators Master Thesis, Lund University, Lund, Sweden, 2010
[8] Yadav, G. G., *et al*., Nanostructure-Based Thermoelectric Conversion: An Insight into the Feasibility and Sustainability for Large-Scale Deployment, *Nanoscale, 3* (2011), 9, pp. 3555-3562
[9] Cadoff, I. B., Miller, E., *Thermoelectric Materials and Devices*, Reinhold Publishing Corporation, New York, USA, 1960
[10] Riffat, S. B., Xioali, M., Thermoelectrics: A Review of Present and Potential Applications, *Applied Thermal Engineering, 23* (2003), 8, pp. 913-935
[11] Rowe, D. M., Thermoelectrics, An Environmentally Friendly Source of Electrical Power, *Renewable Energy, 16* (1999), 1-4, pp. 1251-1265
[12] Yee, S. K., *et al.*, $ per W Metrics for Thermoelectric Power Generation: Beyond ZT, *Energy & Environmental Science, 6* (2013), Jun., pp. 2561-2571
[13] Yazawa, K., Shokouri, A.,, Optimisation of Power and Efficiency of Thermoelectric Devices with Asymmetric Thermal Contacts, *Journal of Applied Physics, 111* (2012), Jan., 024509
[14] Mayer, P. M., Ram. R. J., Optimisation of Heat Sink-Limited Thermoelectric Generators, *Nanoscale and Microscale Thermophysical Engineering, 10* (2006), 2, pp. 143-155
[15] Conklin, J. C., Szybist, J. P., A Highly Efficient Six-Stroke Internal Combustion Engine Cycle with Water Injection for In-Cylinder Exhaust Heat Recovery, *Energy, 35* (2010), 4, pp. 1658-1664
[16] Stobart, R., Weerasinghe, R., Heat Recovery and Bottoming Cycles for SI and CI Engines – A Perspective, SAE paper: 2006-01-0662, 2006
[17] Stobart, R., *et al*., The Potential for Thermoelectric Devices in Passenger Vehicle Applications, SAE paper: 2010-01-0833, 2010
[18] Birkholtz, U., *et al*., Conversion of Waste Exhaust Heat in Automobile Using $FeSi_2$ Thermoelements, *Proceedings*, 7th IEEE International Conference on Thermoelectric Energy Conversion, Arlington, Va.,USA, 1988
[19] Ramade, P., *et al*., Automobile Exhaust Thermo-Electric Generator Design and Performance Analysis, *International Journal of Emerging Technology and Advanced Engineering, 4* (2014), 5, pp. 682-691
[20] Chen, L., *et al*., Performance Optimisation of a Two Stage Semiconductor Thermoelectric-Generator, *Applied Energy, 82* (2005), 4, pp. 300-312
[21] Hendricks, T. J., Integrated Thermoelectric Thermal System Resistance Optimisation to Maximize Power Output in Thermoelectric Energy Recovery Systems, *Materials Research Society Proceedings, 1642* (2014)
[22] Kumar, C. R., *et al*., Experimental Study on Waste Heat Recovery from an Internal Combustion Engine Using Thermoelectric Technology, *Thermal Science, 15* (2011), 4, pp. 1011-1022
[23] Savelli, G., *et al*., Energy Conversion Using New Thermoelectric Generator, *Proceedings*, DTIP of MEMS and MOEMS, Stresa, Italy, 2006
[24] Kuo, K. K., *Principles of Combustion*, John Wiley & Sons, Inc., Hoboken, N. J., USA, 2005
[25] Heywood, J. B., *Internal Combustion Engine Fundamentals*, McGraw-Hill, New York, USA, 1988
[26] Glassman, I., Yetter, R. A., *Combustion,* Academic Press, San Diego, Cal., USA, 1996
[27] Jinhua, W., *et al*., Numerical Study of the Effect of Hydrogen Addition on Methane-Air Mixtures Combustion, *International Journal of Hydrogen Energy, 34* (2009), 2, pp. 1084-1096

[28] Schefer, R. W., Hydrogen Enrichment for Improved Lean Flame Stability, *International Journal of Hydrogen Energy, 28* (2003), 10, pp. 1131-1141
[29] Shirk, M. G., *et al*., Investigation of a Hydrogen-Assisted Combustion System for a Light-Duty Diesel Vehicle, *International Journal of Hydrogen Energy, 33* (2008), 23, pp. 7237-7244
[30] Kumar, M. S., *et al*., Use of Hydrogen to Enhance the Performance of a Vegetable Oil Fuelled Compression Ignition Engine, *International Journal of Hydrogen Energy, 28* (2003), 10, pp. 1143-1154
[31] Choi, G. H., *et al.*, Performance and Emissions Characteristics of a Hydrogen Enriched LPG Internal Combustion Engine at 1400 rpm, *International Journal of Hydrogen Energy, 30* (2005), 1, pp. 77-82

Paper submitted: April 17, 2015
Paper revised: November 11, 2015
Paper accepted: November 19, 2015